ELSEVIER

Chemical Engineering Science 62 (2007) 3589–3594

Chemical Engineering Science

www.elsevier.com/locate/ces

Multi-scale analysis of AFM tip and surface interactions

Haiying Wang[a], Ming Hu[a,b], Nan Liu[a], Mengfen Xia[a,c], Fujiu Ke[a,d], Yilong Bai[a,*]

[a]*State Key Laboratory of Nonlinear Mechanics, Institute of Mechanics, Chinese Academy of Sciences, Beijing 100080, China*
[b]*Graduate School of Chinese Academy of Sciences, Beijing 100039, China*
[c]*Department of Physics, Peking University, Beijing 100871, China*
[d]*Department of Physics, Beihang University, Beijing 100083, China*

Received 1 July 2006; received in revised form 27 November 2006; accepted 30 November 2006
Available online 24 March 2007

Abstract

Thoroughly understanding AFM tip–surface interactions is crucial for many experimental studies and applications. It is important to realize that despite its simple appearance, the system of tip and sample surface involves multiscale interactions. In fact, the system is governed by a combination of molecular force (like the van der Waals force), its macroscopic representations (such as surface force) and gravitational force (a macroscopic force). Hence, in the system, various length scales are operative, from sub-nanoscale (at the molecular level) to the macroscopic scale. By integrating molecular forces into continuum equations, we performed a multiscale analysis and revealed the nonlocality effect between a tip and a rough solid surface and the mechanism governing liquid surface deformation and jumping. The results have several significant implications for practical applications. For instance, nonlocality may affect the measurement accuracy of surface morphology. At the critical state of liquid surface jump, the ratio of the gap between a tip and a liquid dome (δ) over the dome height (y_0) is approximately ($n-4$) (for a large tip), which depends on the power law exponent n of the molecular interaction energy. These findings demonstrate that the multiscale analysis is not only useful but also necessary in the understanding of practical phenomena involving molecular forces.

Keywords: Multiscale; AFM; Tip; Sample; Interaction

1. Introduction

The inventions of the Scanning Tunneling Microscope (STM), Atomic Force Microscope (AFM) and nanoindentation (Binnig et al., 1982, 1986; Oliver and Pharr, 1992) have enabled us to analyze material behavior with nanometer resolutions. Till now, these instruments have been popularly used for materials characterization at the nanometer scale (Mati et al., 1987; Albrecht and Quate, 1987; Meyer and Amer, 1990). In these instruments, tip–surface systems are widely employed. Let us take AFM as an example. In AFM testing, a very sharp tip is dragged across a sample surface. The force acting on the tip causes the position of the tip to change and the change in the vertical position (denoted as "z" axis) reflects the topography of the surface. By collecting the height data for a succession of lines it is possible to form a three-dimensional map of the surface morphology of the sample (Binnig et al., 1986). Therefore, a thorough understanding of the tip–surface interactions in AFM testing is crucial for the correct interpretation of the experimental data.

Many researchers have conducted studies on the system of nanometer tip and sample (Thundat et al., 1992; Ciraci et al., 1990; Paik et al., 1991; Abraham et al., 1988; Sasaki and Tsukada, 1995; Hölscher et al., 2000). The system looks very simple but actually involves multiscale interaction. For instance, when we measure the topography of a dry surface with AFM, the van der Waals, electrostatic, magnetic forces are in operation in the noncontact mode, and the van der Waals force takes the leading role in the contact mode. In addition, if the surface of the sample is covered by a thin water layer, a capillary force exerted by the thin water layer is often present in the test. Actually, the capillary force is the macroscopic representation of the van der Waals interactions between the

* Corresponding author. Tel.: +86 10 62548133; fax: +86 10 62579511.
E-mail address: baiyl@lnm.imech.ac.cn (Y. Bai).

0009-2509/$ - see front matter © 2007 Elsevier Ltd. All rights reserved.
doi:10.1016/j.ces.2006.11.060

atoms of water and air. Therefore, the system is governed by a combination of molecular force (like van der Waals force), its macroscopic representations (such as surface force) and gravitational field force (a macroscopic force). Hence, in the system, various length scales are operative, from sub-nanoscale (at the molecular level) to the macroscopic scale. The multiscale nature of the system causes the interaction between the nanometer tip and sample very complex. And as a result, it remains an open problem and needs to be further investigated. In this paper, we choose the nonlocality effect and the liquid surface deformation in AFM testing as two examples to illustrate the complexity and specificity of the problem.

Although many forces might be involved in AFM testing, for simplicity, we will only consider the van der Waals force in our nonlocality effect study and van der Waals force, gravity and surface tension in our liquid surface deformation analysis. Since both forces at the microscopic scale (van der Waals force) and the macroscopic scale (gravity, surface tension, etc.) are considered, we need to integrate the forces at the microscopic scale into macroscopic equations. In this paper, we will present an approach based on the additivity of van der Waals force to integrate the microscopic force into macroscopic equations. This approach is used to analyze both examples. The results will demonstrate that the multiscale analysis is not only useful but also necessary in the understanding of the practical phenomena involving molecular forces.

2. The additivity of van der Waals force

In order to integrate the van der Waals force at the microscopic scale into continuum equations, a straightforward approach is to use the additivity concept developed by Hamaker (1937).

Van der Waals force includes all intermolecular forces that act between electrically neutral molecules. They can be either repulsive or attractive depending on the distance between the molecules. Hamaker considered the attractive interaction and developed the additivity concept to determine the equations for the van der Waals forces between two bodies (Hamaker, 1937). The additivity concept allows the force to be calculated based on the interaction between individual atoms making up the bodies. Specifically, if the energy of interaction between two atoms separated by a distance r is given as $-C/r^6$, the nonretarded energy of interaction between two bodies with unit volume and containing ρ_1 and ρ_2 atoms, respectively is

$$w^{\mathrm{att}} = -\frac{C\rho_1\rho_2}{r^6} = -\frac{A}{\pi^2 r^6}, \tag{1}$$

where the superscript "att" stands for attractive interaction, $A = \pi^2 C\rho_1\rho_2$ is the Hamaker constant and the van der Waals force between the two bodies is

$$f^{\mathrm{att}} = -\frac{\partial w(r)}{\partial r} = -\frac{6A}{\pi^2 r^7}. \tag{2}$$

In this paper, we consider both attractive and repulsive interactions between molecules in the analysis of the nonlocality effect. The L-J 6-12 pair potential is used as an approximate model for the van der Waals force as a function of distance. Therefore, the energy of interaction between two atoms separated by a distance r is

$$e(r) = \frac{Cr_0^6}{r^{12}} - \frac{C}{r^6}. \tag{3}$$

In Eq. (3), the first term on the right-hand side is related to the repulsive potential and the second term attractive potential. The parameter r_0 is a characteristic length of intermolecular interaction. Similarly, with the potential defined in Eq. (3), the nonretarded energy of interaction between two bodies with unit volume and containing ρ_1 and ρ_2 atoms is

$$w = \frac{A}{\pi^2 r^6}\left(\frac{r_0^6}{r^6} - 1\right). \tag{4}$$

And the corresponding van der Waals force between the two bodies is

$$f = \frac{A}{\pi^2}\left(\frac{12r_0^6}{r^{13}} - \frac{6}{r^7}\right). \tag{5}$$

3. Nonlocality effect on AFM measurement of surface morphology

The locality assumption is a basic assumption in AFM data interpretation. The assumption means that the load acting on the tip is simply a function of the distance between the tip and the point on the sample right opposite to the tip apex, regardless of condition in the vicinity of the point. However, although locality is a very helpful and tractable assumption, nonlocality always exists because of the finite range of intermolecular interactions (Gai et al., 2002).

We start with the investigation of the nonlocality effect by assuming the AFM tip to be a small sphere approaching a specified rough surface, as shown in Fig. 1. The sample surface is an ideally planar surface with sinusoidal asperities of amplitude a and wavelength λ. The sample is semi-infinite in the z direction and infinite in the x and y directions. The surface profile can be described by

$$z_s = a\cos\left(\frac{2\pi}{\lambda}x\right), \tag{6}$$

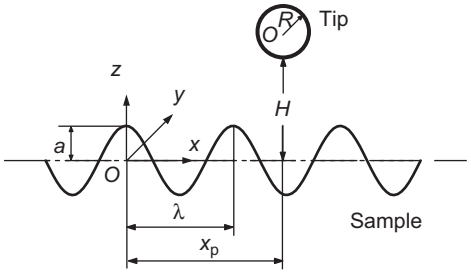

Fig. 1. Schematic diagram of an AFM tip interacting with a specified rough surface.

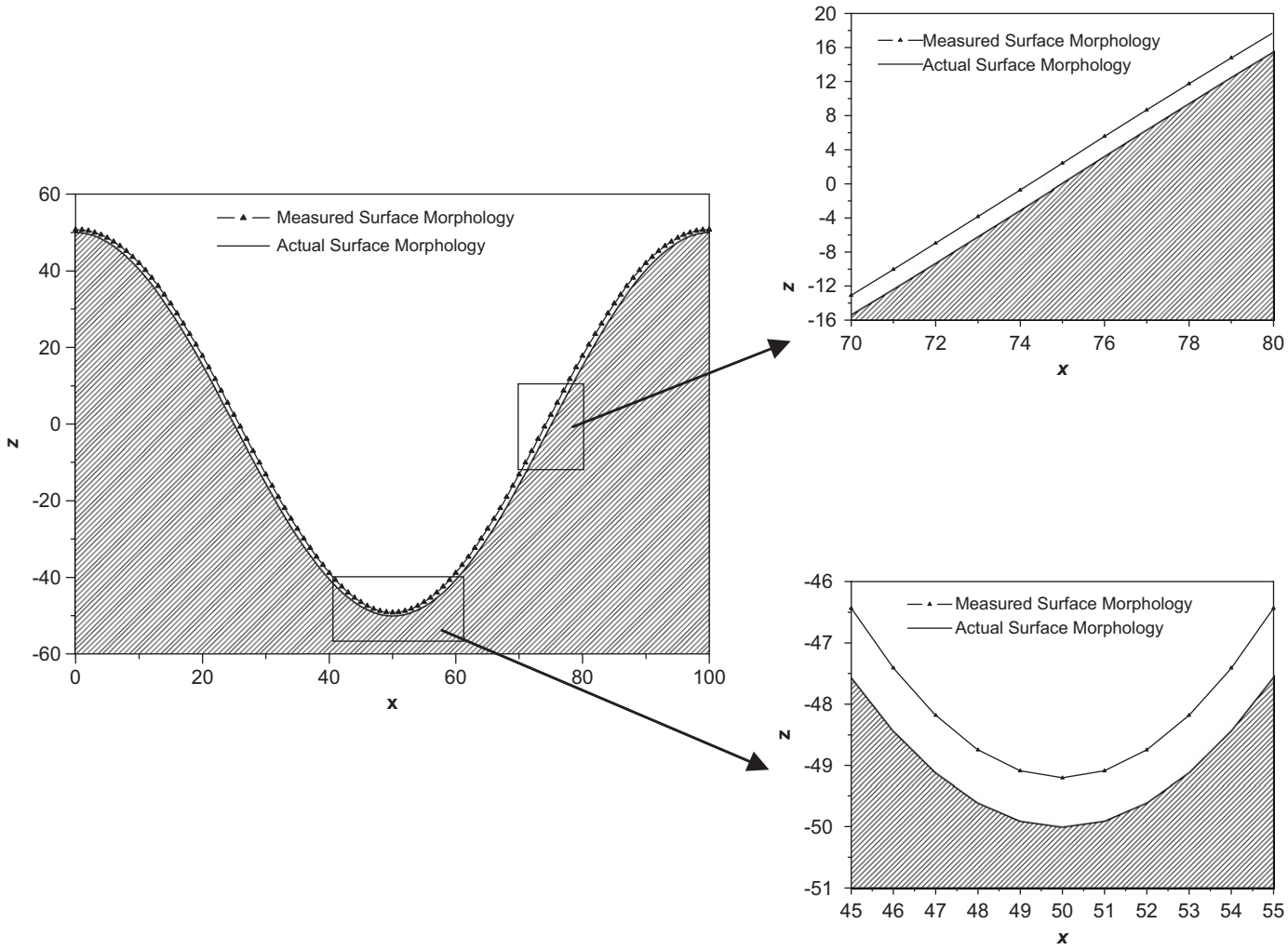

Fig. 2. Comparison of the actual (solid line) and measured (dashdotted line) surface morphologies scanned by a single particle over one asperity period with $a = 50r_0$, $\lambda = 100r_0$ and $f_{\text{fixed}} = 1.953(C/r_0^7)$.

as shown in Fig. 1. For simplicity and convenience, the tip is replaced by a sphere with radius R. The separation between the tip and surface is denoted by H, and x_p is the tip position in the horizontal direction.

With the additivity approach introduced in the last section, we can calculate the energy of interaction between the tip and the sample as W_{ts}^{tot}. In addition, the z component of the interaction force between the tip and the sample can be expressed as

$$f_{ts}^{z} = -\frac{\partial W_{ts}^{\text{tot}}}{\partial H}. \tag{7}$$

As we are primarily interested in the z component of the force in this study, we omit the superscript above and denote the force simply as f_{ts} in the remainder of this paper. The details of the calculation can be found in Hu et al. (2005).

We perform a series of force calculations by choosing a z interval. For a prefixed scanning force f_{fixed}, we may find the root of the equation

$$f_{ts} = f_{\text{fixed}} \tag{8}$$

through the golden search method (Hu et al., 2005; Press et al., 1992). And hence, the AFM image with a constant scanning force of f_{fixed} can be obtained.

Firstly, we consider the case of a tip consisting of a single atom whose size is infinitely small. Now, let the tip be so close to the sample surface that the AFM can work in contact mode. With the assumption of $f_{\text{fixed}} = 1.953(C/r_0^7)$, we can obtain the "measured" morphology scanned by the single-atom tip, as shown in Fig. 2. For comparison, we also include the actual surface morphology of the sample in Fig. 2.

From Fig. 2, we can see that in the case of a single-atom tip, the measured and actual surface morphologies are almost identical, except for a slight difference (see the two insets in Fig. 2). By varying a and λ, we find the difference caused by nonlocality becomes more pronounced when the sample surface becomes rougher (Hu et al., 2005). Therefore, we can conclude that the nonlocality effect on morphology measurement in AFM testing is intrinsic, even with a single-atom tip. However, when the sample surface is not very rough, the nonlocality effect in AFM measurement with a single-atom tip is small and the

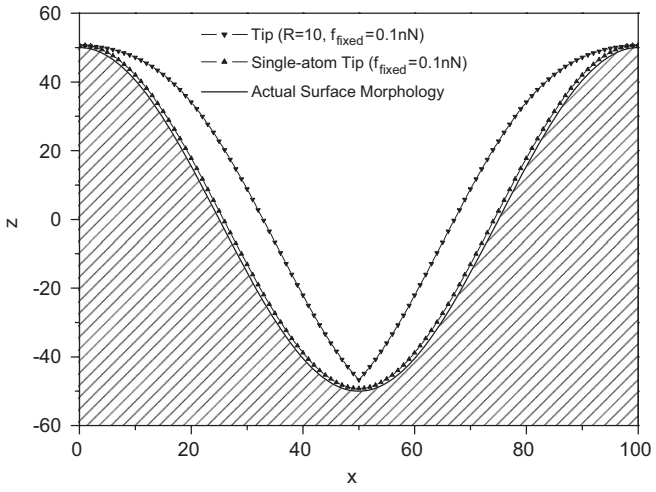

Fig. 3. Comparison of the actual (solid line) and measured (dash-dotted line) surface morphologies scanned by a finite size tip with $R = 10r_0$ over one asperity period with $a = 50r_0$ and $\lambda = 100r_0$ under a constant load of $f_{\text{fixed}} = 1.953C/r_0^7$.

measured results obtained using a locality assumption can be trusted.

We now assume that the spherical tip is not so small, and instead has a finite size of $R = 10r_0$. We can calculate the "measured" surface morphology using the finite size tip, as shown in Fig. 3, which clearly shows that there are significant discrepancies between the measured and the actual surface morphologies. In addition, a comparison between Figs. 2 and 3 demonstrates that the considerable difference between the measured surface morphology and the actual one is mainly induced by the geometrical structure of the sample surface and the finite size of the tip. Therefore, when using a realistic tip with finite size to scan the surface, we must consider the nonlocality effect induced by the AFM tip on the measured surface morphology. We have developed a data processing algorithm—the approaching method to effectively reduce the nonlocality effect in AFM measurement of surface morphology (Hu et al., 2005).

4. Liquid surface deformation and jumping

AFM is often practically operated in air. There will be always some humidity present, therefore, the sample may be covered with a water film (Freund et al., 1999; Colchero et al., 1998). The interaction between the tip and the sample may be greatly influenced by the liquid film, which will definitely affect the test data. To understand the above effect, we need to know how the liquid film deforms and jumps under tip interaction.

Due to the flowability of liquids, this film will no longer remain flat under its interaction with the tip. Therefore, we establish a model shown in Fig. 4 to analyze the deformation and stability of the liquid surface. In this problem, we consider the van der Waals force, gravity and surface tension. The total energy of the system is composed of the liquid surface energy $W_\gamma(y)$, gravitational potential from the mass of the liquid raised above the undeformed state $W_g(y)$, and the energy

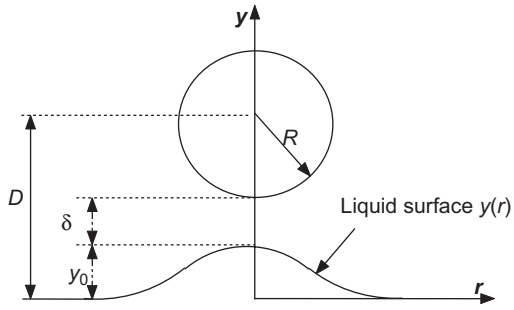

Fig. 4. A schematic illustration of the deformation of a liquid surface.

related to the van der Waals force between the probe tip and the liquid, $W_{\text{vdW}}(y)$. These contributions are functions of the liquid surface shape $y(r)$. It is noticeable that with the additivity of the van der Waals force, the potential between two interacting bodies can be characterized by the Hamaker constant A and the potential between two unit volumes takes the form $w^{\text{att}} = -A/\pi^2 r^6$, as Eq. (1) shows.

By minimizing the total energy functional $W(y) = W_\gamma(y) + W_g(y) + W_{\text{vdW}}(y)$ with respect to the shape function $y(r)$, we obtain the governing equation for the shape of the liquid surface $y(r)$ in the form of

$$\frac{1}{r}\frac{\mathrm{d}}{\mathrm{d}r}\left[r\frac{y'}{\left(1+y'^2\right)^{1/2}}\right] + \frac{4}{3\pi}\frac{A}{\gamma_{LV}} \times \frac{R^3}{[(D-y)^2 + r^2 - R^2]^3} - \frac{\rho g}{\gamma_{LV}}y = 0, \tag{9}$$

with the boundary conditions of

$$y'(r=0) = 0 \quad \text{and} \tag{10}$$

$$\lim_{r\to\infty} y(r) = 0. \tag{11}$$

In Eq. (9), ρ is the liquid density, g is the gravitational acceleration, γ_{LV} is the surface tension coefficient of the liquid, R is the radius of the probe tip, and D is the distance between the center of the sphere probe tip and the undeformed liquid surface (Fig. 4). The terms in Eq. (9) can be seen as the balance of the following forces: surface tension (the first term), van der Waals force (the second term), and gravity (the third term).

It is worth noting that in Eq. (9), there are several length scales: the capillary length ($\lambda = \sqrt{\gamma_{LV}/\rho g}$) defined as the square root of the ratio of surface tension over gravity is on the order of mm; the other intrinsic length scale ($\sqrt{A/\gamma_{LV}}$) characterizing the competition between the intermolecular force and the surface tension is on the order of nm; the tip radius R and the distance between the tip and the original surface is on the order of submicron or nm. Certainly, owing to the large range of these length scales ($\sim 10^6$) this is a multiscale problem and it is hard to know which factors dominate the deformation of the liquid surface.

Eq. (9) can be solved with an asymptotic method (Liu et al., 2005; Liu, 2005). The maximum height of the liquid surface

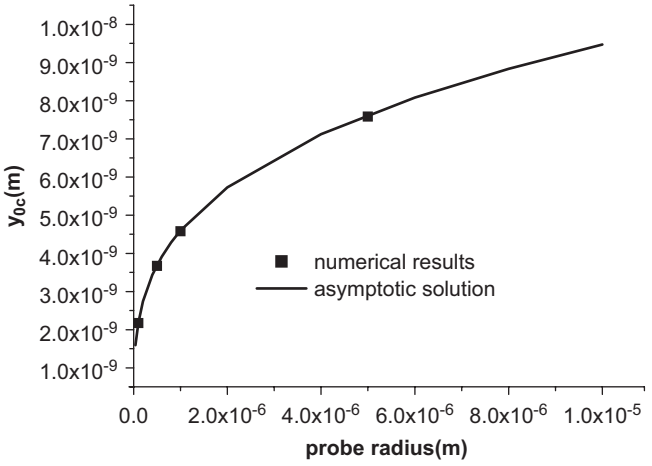

Fig. 5. The variation of the surface height (y_0) with various tip radius (R) at the critical state ($A = 10^{-19}$J, $n = 6$, $\rho = 10^3$ Kg/m^3, $g = 9.8$ m/s^2, $\gamma_{LV} = 0.072$ N/m).

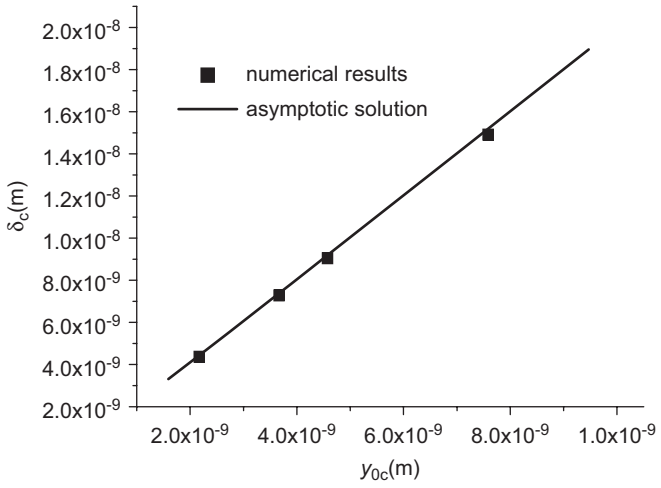

Fig. 6. The relationship between the gap between the tip and surface (δ) and the surface height (y_0) at the critical state, when the surface is about to jump up, under van der Waals interaction. Clearly, the ratio δ/y_0 remains a constant of $2 = n - 4$. ($A = 10^{-19}$J, $n = 6$, $\rho = 10^3$ Kg/m^3, $R = 10^{-7}$ m, $g = 9.8$ m/s^2, $\gamma_{LV} = 0.072$ N/m).

$y_0 = y(r = 0)$ can be given as

$$y_0 = \frac{AR^3}{3\pi\gamma_{LV}} \frac{1}{[(D - y_0)^2 - R^2]^2} \times \left(\frac{1}{2} + \ln \left[\frac{2\lambda}{\sqrt{(D - y_0)^2 - R^2}} \right] - Eu \right). \quad (12)$$

Eq. (12) shows that the vertical scale of the liquid dome is not merely governed by molecular force but mainly by a combination of van der Waals force, surface tension and tip radius. Actually, a dimensional analysis on Eq. (9) also gives $y_0 \propto \sqrt[3]{AR/\gamma_{LV}}$, almost independent of gravity. That is reasonable, since the liquid film is very thin and the gravity is negligible when compared with the surface tension. In typical AFM tests, the probe radius varies from nanometers to submicrons. Hence, the height of the liquid dome is on the order of nanometers.

We can also analyze the stability of the solution of y_0 (Eq. (12)) with respect to perturbations in D to find out the critical state when the liquid dome jumps up to the tip. Fig. 5 demonstrates the variation of the surface height at the critical state y_{0c} with tip radius R under van der Waals interaction (Liu, 2005).

Further investigation on y_{0c} and δ_c shows that, if the molecular interaction potential can be described by a power law with exponent n, the ratio of the gap between the tip and the liquid dome over the dome height at the critical state is determined by the exponent. For a relatively large tip (like 1 μm), the ratio is about $(n - 4)$ (see Fig. 6); while for a very small tip, the ratio is about $(n - 2)$. So, perhaps, one can obtain the intermolecular power exponent n by simply monitoring the critical state of the liquid surface (Liu, 2005).

5. Summary

This paper has shown that multiscale analyses are needed in order to correctly and accurately interpret experimental data on tip–sample interaction in AFM testing. Taking advantage of the additivity of the van der Waals force, we have integrated microscopic forces into macroscopic equations in a theoretical analysis of the interaction between an AFM tip and a sample surface. This method allows the nonlocality effect and the liquid surface deformation and jumping process to be analyzed.

The nonlocality effect on the morphology measurement of a sample surface results from both the intrinsic characteristic length scales of intermolecular interactions and the finite tip size. Hence, even for a single atom probe, nonlocality may still have an significant effect on the measurement. The finite size of the probe can make the nonlocality effect more severe.

Liquid surface deformation and jumping during the interaction between a probe and a measured surface involves several length scales. The height of the liquid dome is mainly governed by a combination of van der Waals force, surface tension and tip radius as $y_0 \propto \sqrt[3]{AR/\gamma}$. For a typical AFM tip, the height is on the order of nanometers. More interestingly, the ratio of the gap between a tip and a liquid dome (δ) over the dome height (y_0) at the critical state, is related to the power index n of the interaction energy. For a large tip, the ratio is approximately $(n - 4)$; while for a very small tip, the ratio is $(n - 2)$.

Acknowledgement

This work is supported by the CAS innovation program (KJCX-SW-L08, KJCX2-YW-M04) and the National Natural Science Foundation of China (10432050).

References

Abraham, F.F., Batra, I.-P., Ciraci, S., 1988. Effect of tip profile on atomic force microscopy images: a model study. Physical Review Letters 60 (13), 1314–1317.

Albrecht, T.R., Quate, C.F., 1987. Atomic resolution imaging of a nonconductor by atomic force microscopy. Journal of Applied Physics 62 (7), 2599–2602.

Binnig, G., Rohrer, H., Gerber, C., Heibel, E., 1982. Tunnelling through a controllable vacuum gap. Applied Physics Letters 40 (2), 178–180.

Binnig, G., Quate, C.F., Gerber, Ch., 1986. Atomic force microscope. Physical Review Letters 56 (9), 930–933.

Ciraci, S., Baratoff, A., Batra, I.P., 1990. Tip-sample interaction effects in scanning-tunneling and atomic force microscopy. Physical Review B 41 (5), 2763–2775.

Colchero, J., Storch, A., Luna, M., Herrero, J. G., Baro, A. M., 1998. Observation of liquid neck formation with scanning force microscopy techniques. Langmuir 14 (9), 2230–2234.

Freund, J., Halbritter, J., and Horber, J.K.H., 1999. How dry are dried samples? Water adsorption measured by STM. Microscopy Research and Technique 44 (5), 327–338.

Gai, Z., Wu, B., Pierce, J.P., Farnan, G.A., Shu, D.J., Wang, M., Zhang, Z.Y., Shen, J., 2002. Self-assembly of nanometer-scale magnetic dots with narrow size distributions on an insulating substrate. Physical Review Letters 89 (23), 235–502.

Hamaker, H.C., 1937. The London-van der waals attraction between spherical particles. Physica 4 (10), 1058–1072.

Hölscher, H., Allers, W., Schwarz, U.D., Schwarz, A., Wiesendanger, R., 2000. Interpretation of 'True atomic resolution' images of graphite (0 0 0 1) in noncontact atomic force microscopy. Physical Review B 62 (10), 6967–6970.

Hu, M., Wang, H.Y., Xia, M.F., Ke, F.J., Bai, Y.L., 2005. Nonlocality effect in atomic force microscopy measurement and its reduction by an approaching method. Transactions of ASME Journal of Engineering Materials Technology 127, 444–450.

Liu, N., 2005. The distortion and instability of liquid surface induced by a sub-microscale probe. Master's Thesis, Institute of Mechanics, Chinese Academy of Sciences, Beijing.

Liu, N., Bai, Y.L., Xia, M.F., Ke, F.J., 2005. Combined effect of surface tension, gravity and van der Waals force induced by a non-contact probe tip on the shape of liquid surface. Chinese Physics Letters 22 (8), 2012–2015.

Mati, O., Drake, B., Hansma, P.K., 1987. Atomic force microscopy of liquid-covered surfaces: atomic resolution images. Applied Physics Letters 51 (7), 484–486.

Meyer, M., Amer, N.M., 1990. Optical-beam-deflection atomic force microscopy: the NaCl (0 0 1) surface. Applied Physics Letters 56 (21), 2100–2101.

Oliver, W.C., Pharr, G.M., 1992. An improved technique for determining hardness and elastic modulus using load and displacement sensing indentation experiments. Journal of Materials Research 7, 1564–1583.

Paik, S.M., Kim, S., Schuller, I.K., 1991. Method of determining tip structure in atomic force microscopy. Physical Review B 44 (7), 3272–3276.

Press, W.H., Teukolsky, S.A., Vetterling, W.T., Flannery, B.P., 1992. Numerical Recipes in Fortran 77: The Art of Scientific Computing (vol 1 of Fortran numerical recipes). Cambridge University Press, Cambridge, UK.

Sasaki, N., Tsukada, M., 1995. Effect of the tip structure on atomic-force microscopy. Physical Review B 52 (10), 8471–8482.

Thundat, T., Warmack, R.J., Allison, D.P., Bottomley, L.A., Lourenco, A.J., Ferrell, T.L., 1992. Atomic force microscopy of deoxyribonucleic acid strands absorbed on mica: the effect of humidity on apparent width and image contrast. Journal of Vacuum Science and Technology A 10 (4), 630–635.